

# Enhancement of Barrier Properties in Organic Coatings using Nanocomposites

D. Greenfield and F. Clegg

*Materials Research Institute, Sheffield Hallam University, Sheffield S1 1WB,*

[d.greenfield@shu.ac.uk](mailto:d.greenfield@shu.ac.uk)

## Abstract

Organic/inorganic nanocomposites have aroused much interest in recent years because of the enhancement of physical properties that have been achieved by dispersing nanometre-scaled, inorganic additives into an organic polymer matrix. One application of this technology is as a gas barrier for films in the packaging industry. As the size of these additives is less than the wavelength of visible light, an attractive characteristic of this approach is the potential reduce gas transmission rates without compromising the transparency of the packaging film. The main thrust of this research is to investigate affects on the barrier properties of organic coatings resulting from application of this technology. Traditionally, the barrier properties of anticorrosive polymer coatings have been enhanced through the incorporation of micrometre-scaled non-permeable pigments such as talc, micaceous iron oxide or glass flake. This paper describes the affect of including intercalated and exfoliated nanoclays into a range of coatings. Furthermore, work carried out to look for synergies between these novel pigments and more traditional micrometer-scaled barrier pigments is presented.

**Keywords:** Barrier coatings, Organic/inorganic nanocomposite

## Introduction

The work reported here is concerned with the incorporation of clay nanoparticles into a polymeric coating, forming an organic / inorganic nanocomposite. The clays used were commercially available organo-clays. This material comprises of many clay layers one nanometre thick stacked together. In their natural form, the faces of these platelets are coated with inorganic cations, typically Na Ca and Mg. These cations are hydrated and hence incompatible with many polymers. It has been known since the 1930's that these

cations can be exchanged for long alkyl chain surfactants. This renders the surface of the clay organo-philic and, using different structures, can optimise the interaction between clay and polymer.

This process can result in one of three modes of clay dispersion: intercalated, ordered exfoliated and disordered exfoliated. One of the principle factors affecting the degree of dispersion of the clay is the rate of cure of the polymer [1]. Figure 1 shows how nanocomposites differ from conventional composites and that different types of nanocomposite can be formed. It also identifies the clay layer, the clay gallery and the

Organo-treatment of the clay. All of these features can influence the type of nanocomposites formed. The formation of an exfoliated nanocomposite requires polymerisation to occur rapidly within the gallery between the clay layers. The term nanoparticle is reserved for a dispersed inorganic phase which has no organo-modifier associated with it. The degree of dispersion of the clays was assessed by X-ray diffraction. This is achieved by monitoring the intensity and positioning of the  $d_{001}$  spacing, which reports the distance between stacks of parallel clay sheets [2].

The nanocomposite coatings studied in this work used two different resin systems, epoxy and polyester. Both coatings were two-pack systems and each represented the base resins of commercial paint systems used for anticorrosive applications.

## Results and Discussion

### X-ray Diffraction and Characterisation

The results of the XRD analysis of the degree of dispersion of the nanoclays in the different polymers is presented in Figure 2 to Figure 4, which illustrate the degree of dispersion achieved for the different nanocomposite systems investigated.

Different nanoclays were chosen for their ability to disperse in each base resin. Figure 2 is included to demonstrate that the XRD traces collected from a pressed powder sample of clay, using  $\text{Cr-K}\alpha$  radiation, exhibited a strong  $d_{001}$  peak at  $7.4^\circ 2\theta$  which represents a basal spacing of 1.77 nm. When 15 wt% clay was mixed with polyester a peak at  $3.2^\circ 2\theta$  ( $d_{001} = 4.10$  nm) was observed. This expansion from 1.77 to 4.10 nm proved that the polymer was intercalated. The addition of 15 wt% nanofiller was chosen to demonstrate that the XRD technique could detect the diffraction peak for the polymer swollen clay present in the nanocomposite. The presence of a strong, well defined peak at this angle, together with the

002 peak near  $6.8^\circ 2\theta$ , demonstrates the formation of an ordered, intercalated nanocomposite.

Figure 3 compares the XRD trace for a powdered sample of clay with that for polyester nanocomposites containing 1, 3 and 5 wt% clay. These traces do not display any definite diffraction peaks at low angle, thus qualifying as 'XRD silent' nanocomposites, but the baseline at low  $2\theta$  increased proportional to the amount of expanded clay present.

The XRD traces for composites containing 18 wt% of glass flake together with 1, 3 and 5 wt% clay (Figure 4) demonstrated that the glass flake exerted some influence on the dispersion of the nanofiller in that the addition of glass flake made the peak for the expanded clay more evident at 3 and 5 wt% C30B. Nonetheless, the degree of dispersion was very favourable. Figure 5 shows that powdered clay used in the epoxy nanocomposite coating exhibits a strong peak at  $7.1^\circ 2\theta$  ( $d_{001} = 1.87$  nm). When dispersed in the epoxy matrix a peak at  $3.9^\circ 2\theta$  ( $d_{001} = 3.40$  nm) was evident suggesting that this clay had expanded in the presence of epoxy but not as much as it did in the polyester. Given that the peak shape was quite symmetrical and that there was no increased baseline at low angles – it is likely that this system formed an ordered nanocomposite with some exfoliation.

Comparison of Figure 5 and Figure 6 clearly show that the presence of 18 wt% glass flake had little effect on the dispersion of the selected nanofiller in the epoxy resin.

## AC Impedance Spectroscopy

Having characterised the nanocomposites in terms of their degree of clay dispersion, the next stage of the experimental program proceeded to electrochemical assessment of the different coating systems.

The nanocomposite coating systems have been characterised through the use of EIS: a polyester system, incorporating 1, 3 and 5 wt% clay and an epoxy with the same loadings of clay. In addition, the same nanocomposite materials have been evaluated with the addition of glass flake, in order to determine whether any synergistic action of micro and nanoscaled barrier pigments could be identified. The characteristics of the coatings used to rank them as anti-corrosives were the pore resistance ( $R_p$ ), which indicates the affect of the coating's porosity on the barrier effect and the charge transfer resistance ( $R_{ct}$ ), which describes the electrochemical activity and hence the level of corrosion occurring on the metal surface. The variations of  $R_p$  and  $R_{ct}$  with time, both with and without the addition of glass flake, are presented in Figure 7 to Figure 14 for both the epoxy and the polyester systems.

Examination of Figure 7 to Figure 10 shows that, for the polyester system, there is little impact on the values of  $R_p$  due to the addition of the clay nanoparticles either with or without the addition of glass flake. However, it does seem that  $R_p$  is adversely affected in the epoxy system by the incorporation of glass flake: the values of  $R_p$  remain above  $105 \Omega$ , whereas the coating with glass flake falls below  $105 \Omega$  for the longer exposure times. These lower values for  $R_p$  in the epoxy system could be attributed to poor wetting of the glass flake by the polymer.

On the other hand, the values of  $R_{ct}$  illustrated in Figure 11 to Figure 14, indicate there is a marked improvement of the effectiveness of the coatings, resulting from the incorporation of the nanoclays.

A marked improvement in the properties of the epoxy coating is displayed by the  $R_{ct}$  values in Figure 11. Here the addition of 3% clay yields an improvement of the  $R_{ct}$  value by two orders of magnitude. Figure 12 identifies synergy between glass flake and all concentrations of nanoclay considered but the best results were obtained with 3% nanoclay, yielding a 2–3 order of magnitude improvement in  $R_{ct}$ .

The graph in Figure 13, polyester nanocomposite without glass flake, shows an improvement of the  $R_{ct}$  values for all clay loadings. The results suggest that without glass flake, the addition of 1% nanoclay would be sufficient to produce an improvement in the barrier properties of this system. Examination of Figure 14, which shows the results for a polyester/clay nanocomposite system with the addition of glass flake, shows that the properties of this system are also improved by the incorporation of the nanoclays. For this coating system, both the 3% and 5% loading of clay produced an improvement in the charge transfer resistance by almost one order of magnitude.

## Conclusions

Two organic/inorganic nanocomposite coatings have been evaluated for their anticorrosive properties. In both cases, the protective ability of the coatings is enhanced by appropriate levels of a suitable nanoclay. However, the most impressive improvements occur due to the synergistic effect of nanoclays used in conjunction with micro-scaled glass flake additives.

## Acknowledgments

This work has been funded through a European Union CRAFT project, number G5ST-CT-2002-50213.

## References

1. 'Synthesis and characterisation of layered silicate-epoxy nanocomposites', P.B. Messersmith and E.P. Giannelis, Chem Mater, 6, pp 1719-1725, 1994.
2. 'X-ray powder diffraction of polymer/layered silicate nanocomposites: model and practice', R.A. Vaia and W. Liu, Journal of Polymer Science Part B: Polymer Physics, 40, 15, pp 1590-1600, 2002.

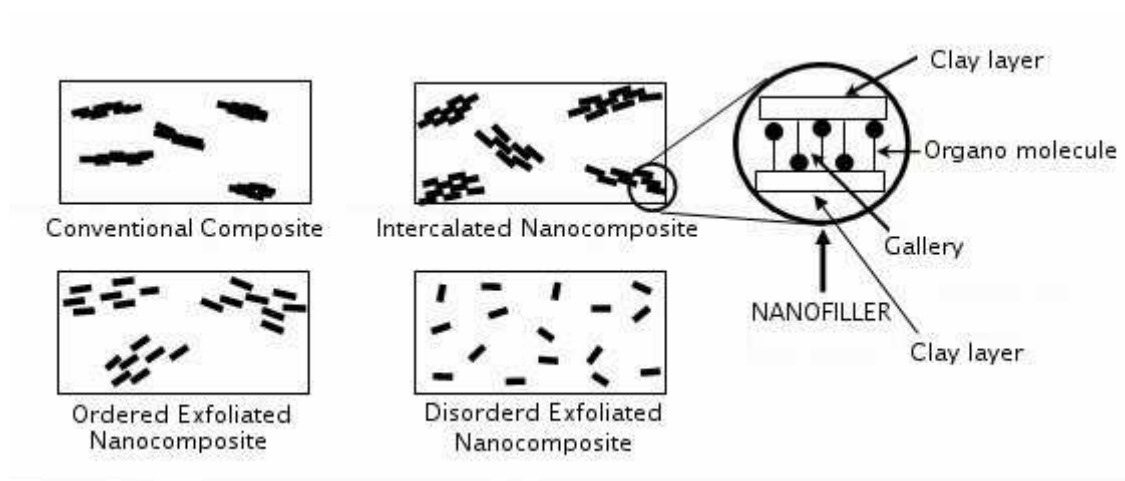


Figure 1: Schematic representation of the three different states of dispersion possible with nanofillers

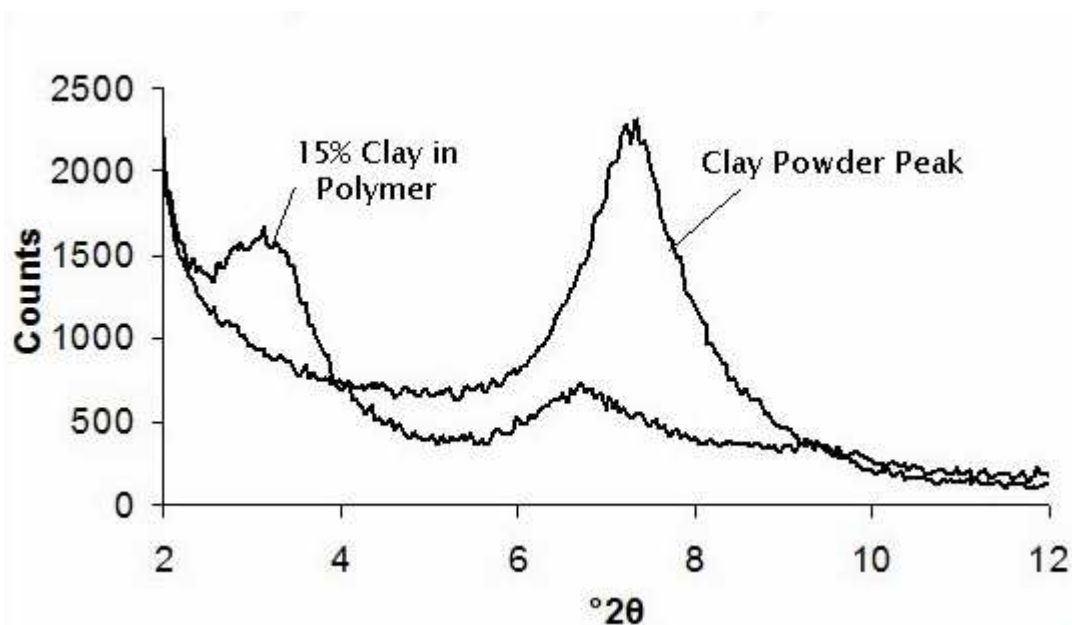


Figure 2: XRD Spectra of pressed clay powder compared to 15 wt% clay dispersed in polyester resin.

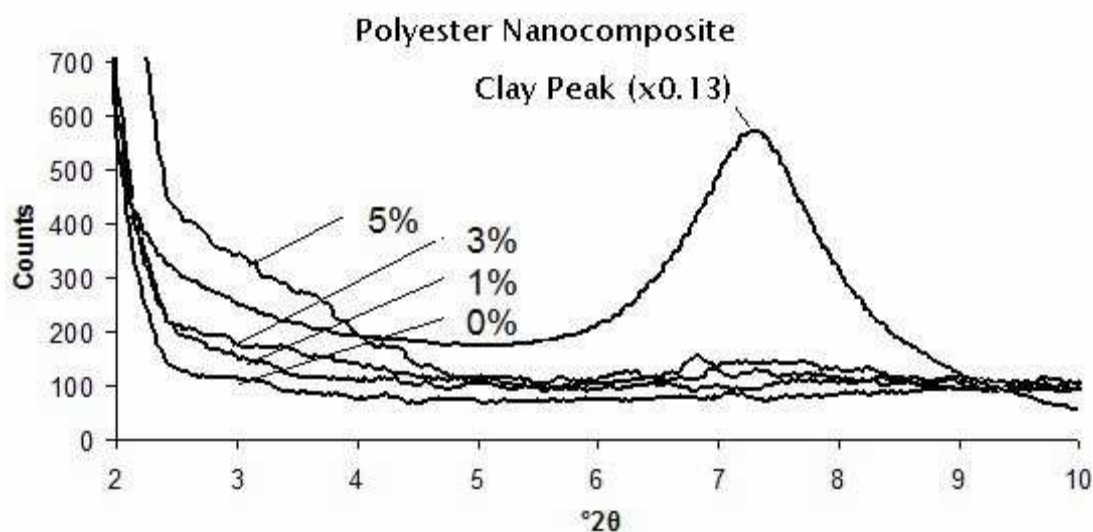


Figure 3: XRD spectra for polyester nanocomposite system



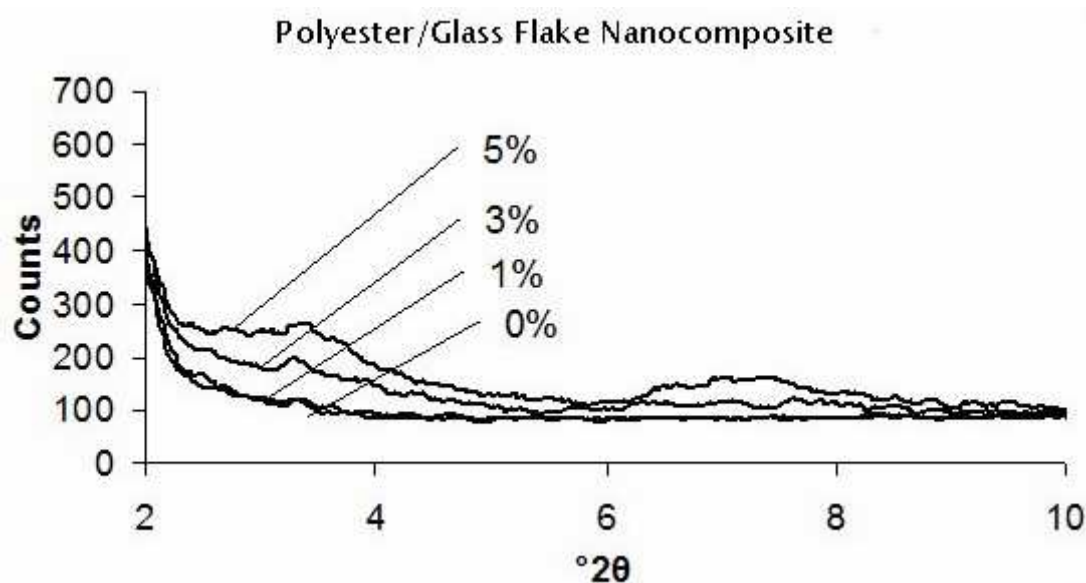


Figure 4: XRD spectra for polyester/glass flake nanocomposite system

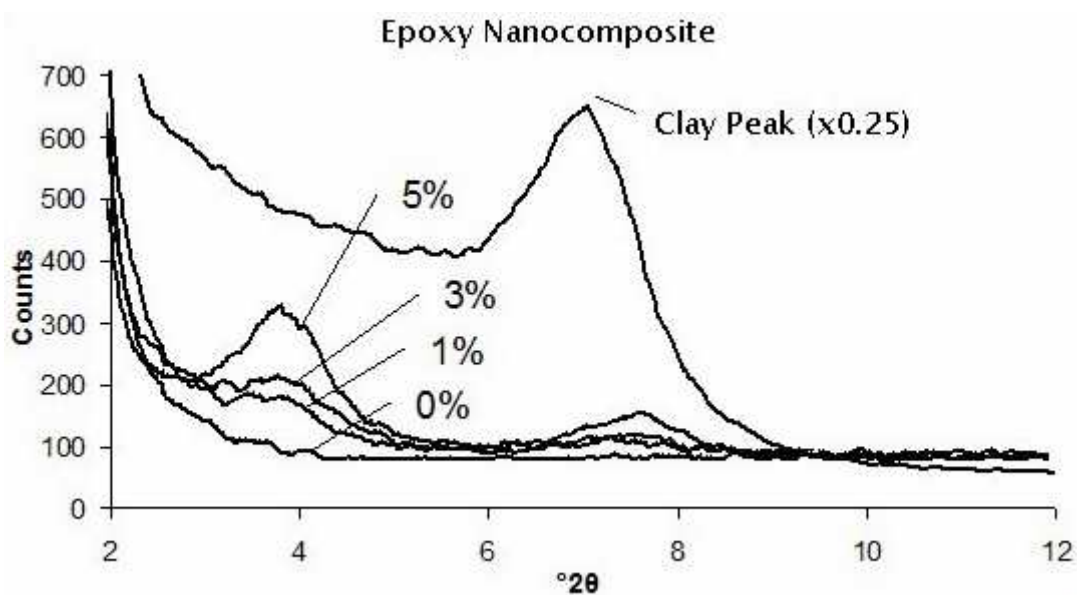


Figure 5: XRD spectra for epoxy nanocomposite system

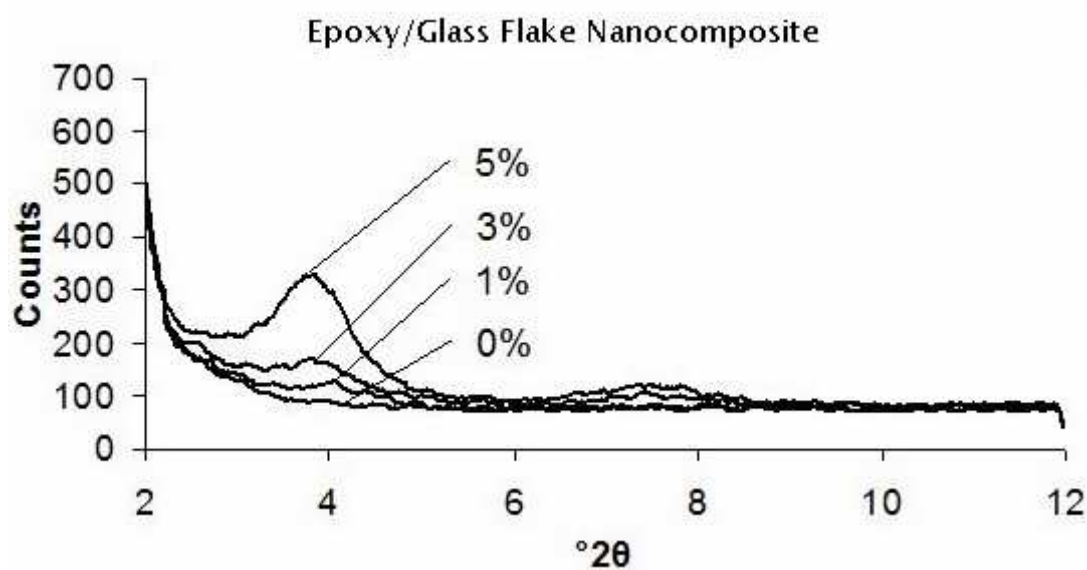


Figure 6: XRD spectra for epoxy/glass flake nanocomposite system

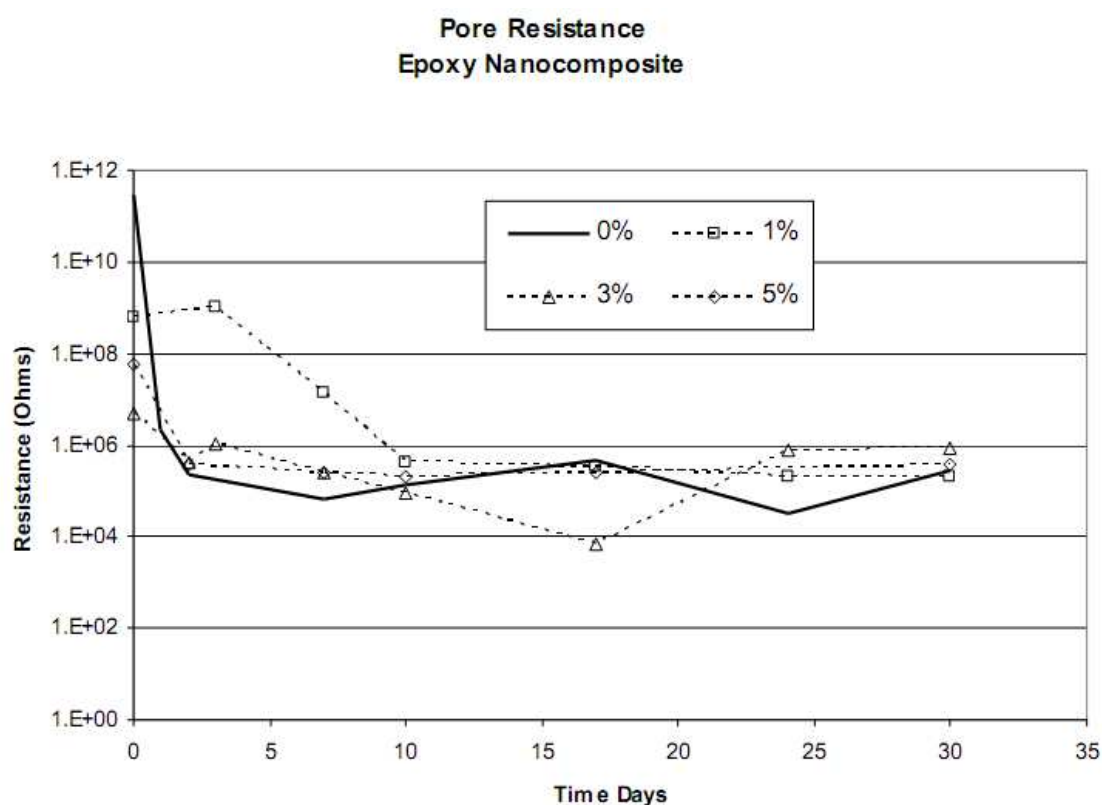


Figure 7: Time resolved pore resistance values for epoxy nanocomposite coating



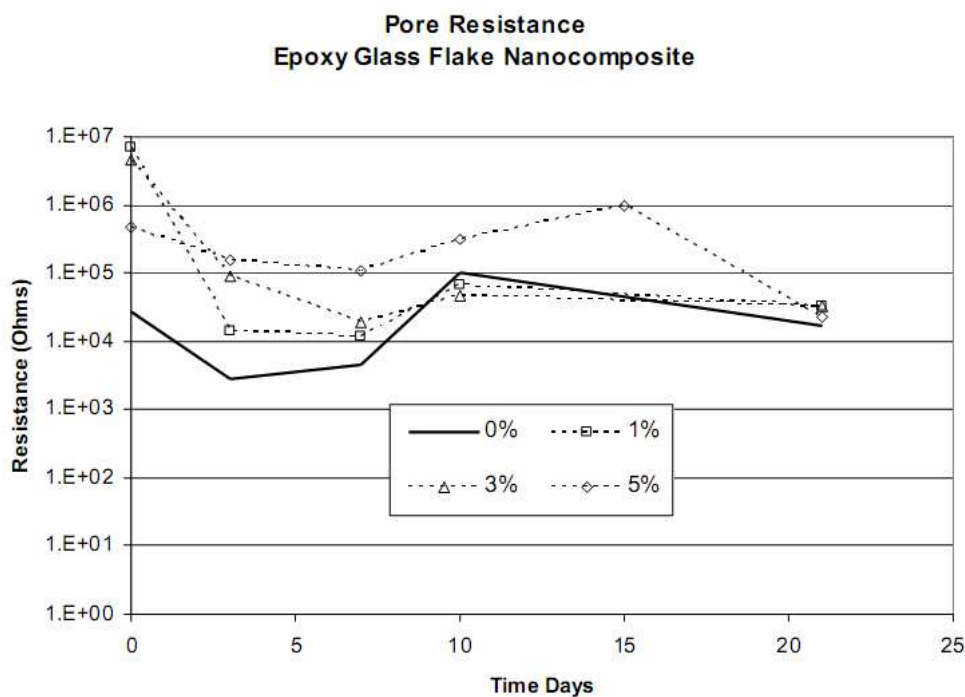


Figure 8: Time resolved pore resistance values for epoxy/glass flake nanocomposite coating

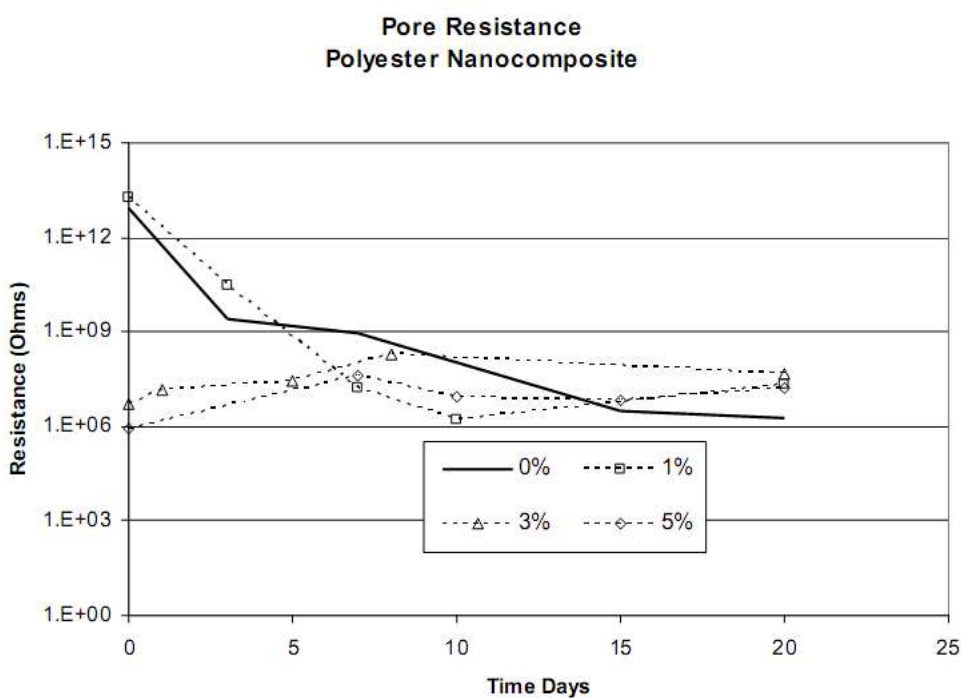


Figure 9: Time resolved pore resistance values for polyester nanocomposite coating

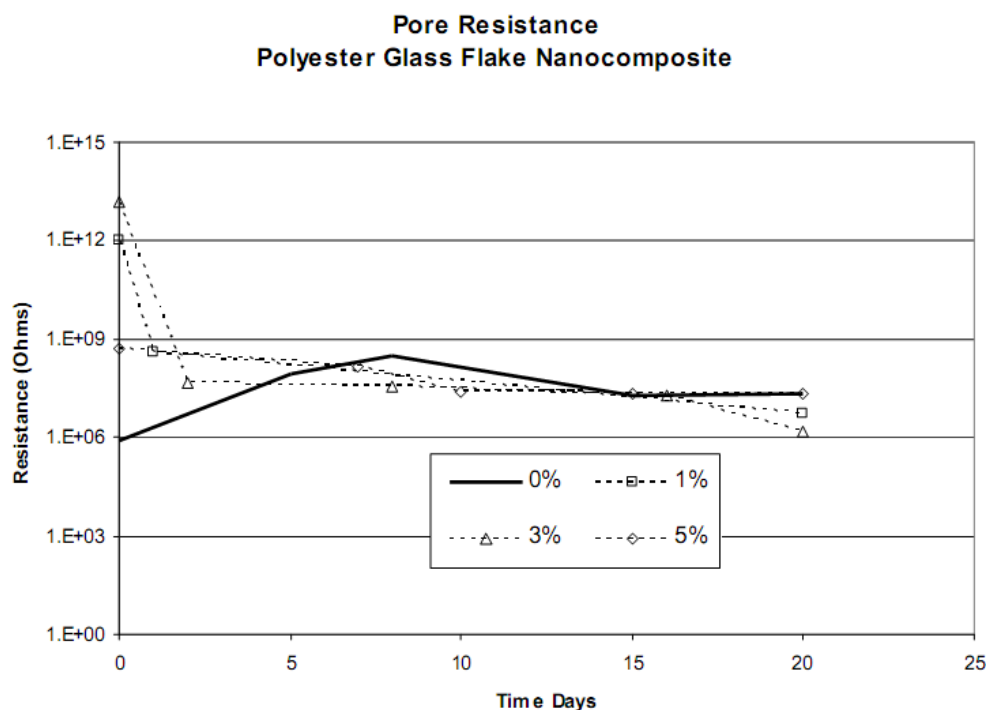


Figure 10: Time resolved pore resistance values for polyester/glass flake nanocomposite coating

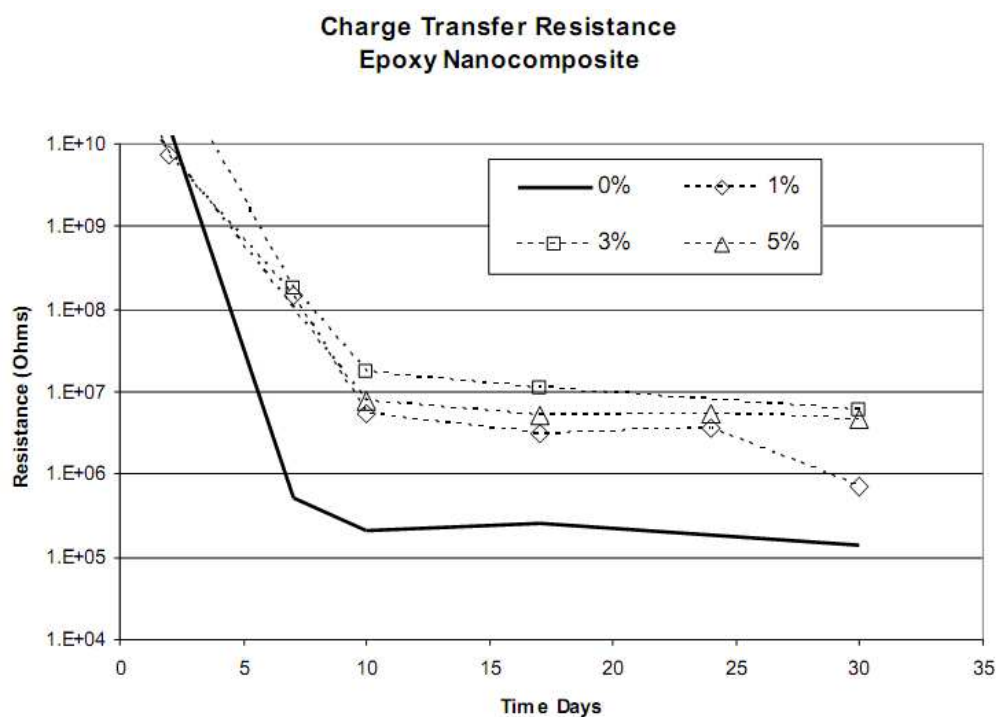


Figure 11: Time resolved charge transfer resistance for epoxy nanocomposite coating

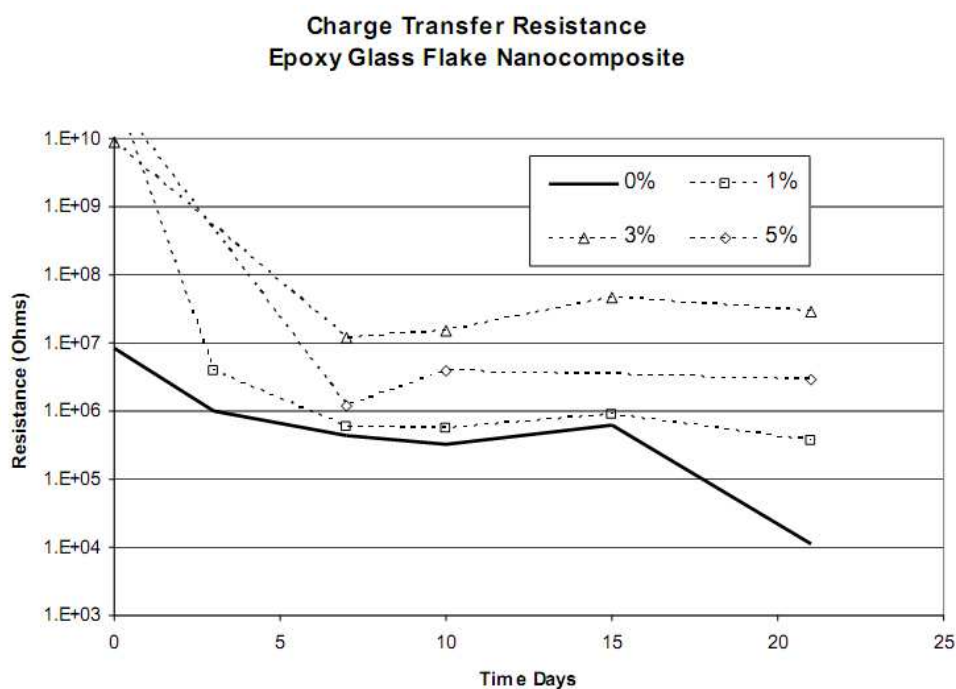


Figure 12: Time resolved charge transfer resistance values for epoxy/glass flake nanocomposite coating

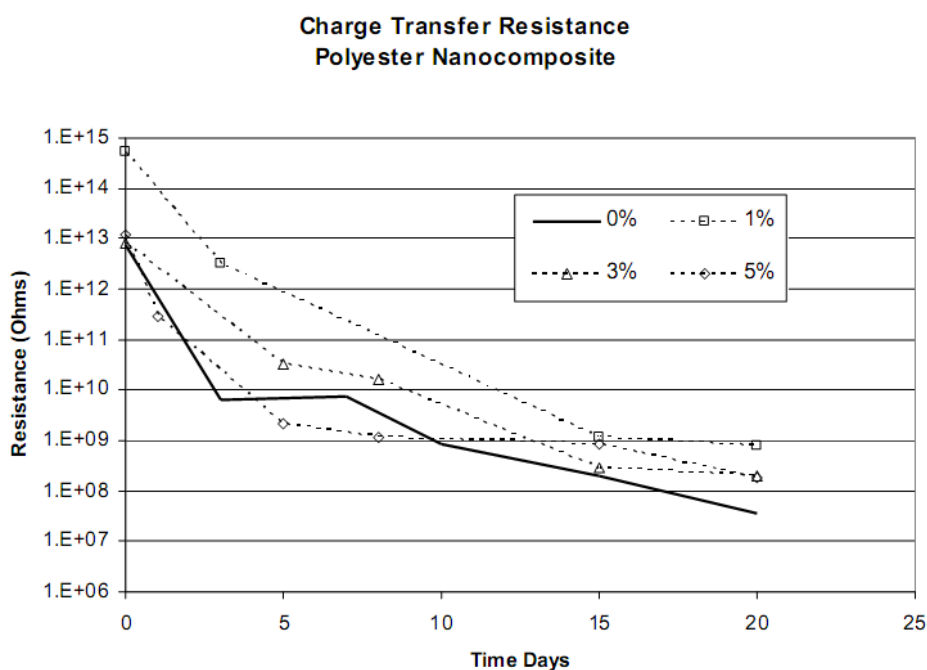


Figure 13: Time resolved charge transfer values for polyester nanocomposite coating

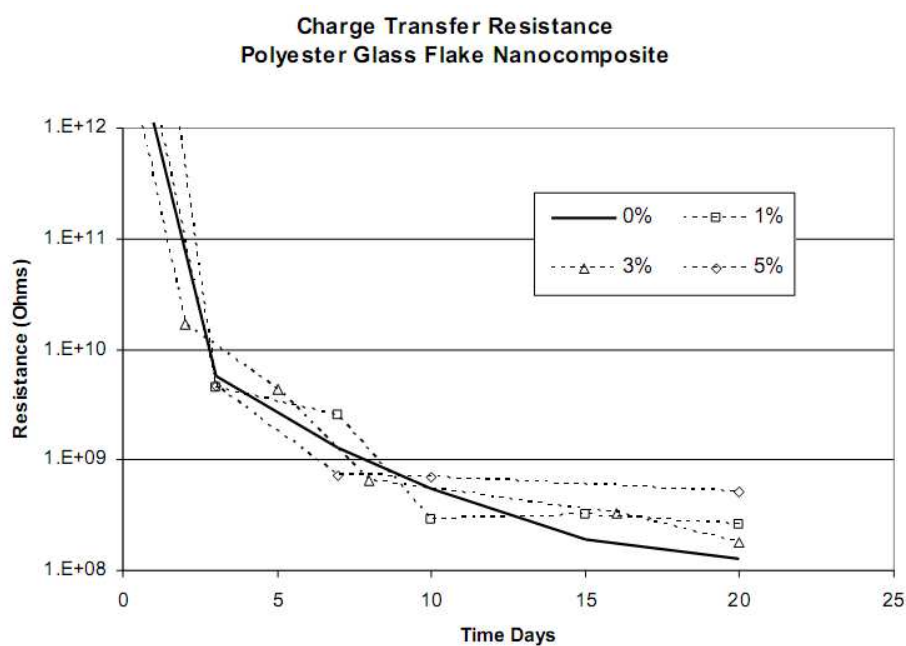


Figure 14: Time resolved charge transfer values for polyester/glass flake nanocomposite coating